The Boston Retinal Prosthesis

A 15-Channel Hermetic Wireless Neural Stimulator

Shawn K. Kelly, Douglas B. Shire, Patrick Doyle, Marcus D. Gingerich, William A. Drohan, Joseph F. Rizzo, III
Boston VA Healthcare System
Boston, MA, USA
skkelly@alum.mit.edu

Jinghua Chen
Massachusetts Eye and Ear Infirmary
Boston, MA USA

Luke S. Theogarajan
University of California
Santa Barbara, CA, USA

Stuart F. Cogan
EIC Laboratories
Norwood, MA USA

John L. Wyatt
Massachusetts Institute of Technology
Cambridge, MA, USA

***Abstract*— A miniaturized, hermetically-encased, wirelessly-operated retinal prosthesis has been developed for pre-clinical studies in Yucatan minipig animal models. The prosthesis attaches conformally to the outside of the eye and drives a microfabricated thin-film polyimide stimulating electrode array with sputtered iridium oxide electrodes. This array is implanted in the subretinal space using a specially-designed ab externo surgical technique that uses the retina to hold the array in place while leaving the bulk of the prosthesis outside the eye. The implanted device includes a hermetic titanium case containing a 15-channel stimulator chip and discrete circuit components. Feedthroughs from the case connect to secondary power- and data-receiving coils. In addition, long-term in vitro pulse testing was performed on the electrodes to ensure that their lifetime would match that of the hermetic case. The final assembly was tested in vitro to verify wireless operation of the system in biological saline using a custom RF transmitter circuit and primary coils. Stimulation pulse strength, duration and frequency were programmed wirelessly using a custom graphical user interface. Operation of the retinal implant has been verified in vivo in two pigs for up to five and a half months by measuring stimulus artifact on the eye surface using a contact lens electrode.**

Keywords-biomedical engineering; biomedical electrodes; bioelectric potentials; neuromuscular stimulation; iridium; integrated circuit design; telemetry

I. INTRODUCTION

Retinal prostheses are actively being developed by a number of groups worldwide [1]–[13]. These devices aim to restore visual function lost due to degenerative retinal diseases such as retinitis pigmentosa (RP) and age-related macular degeneration (AMD). These conditions cause a gradual loss of photoreceptors, yet a substantial fraction of the retinal ganglion cells remain, forming intact neural pathways from the retina to the visual cortex. The prevalence of RP is approximately 1 in every 4000 live births, and there are approximately 1,700,000 affected individuals worldwide. AMD is the leading cause of blindness in the developed world, with roughly 2 million affected patients in the United States alone. This number is expected to increase by 50% by the year 2020 as the population ages [14]. The best existing treatments slow the progress of these diseases, but no cure is known. While there is evidence that significant reorganization of the retina occurs after the loss of input signals from the photoreceptors [15], our group and others have nevertheless shown that focal electrical stimulation of retinal ganglion cells yields responses corresponding to the strength and location of the stimuli (e.g., [16]).

To test the retinal prosthesis concept, our group performed six acute human retinal stimulation trials. Thin-film microfabricated electrode arrays were surgically inserted into the subjects' eyes, resting on or just above the epiretinal surface, each with a tail extending outside the eye to connect to an external stimulator system [17]. Stimulation current pulses were delivered, and subjects reported their perceptions. The electrode array was removed after a few hours. Subjects reported visual percepts, including spots and lines, but even the best percepts reported were not as detailed as we had hoped [3], [4]. It became evident to our team after these studies that a chronically implantable device was required to allow patients to adapt to this artificial stimulation and fully explore the prospects of restoring useful vision.

Other groups are also actively engaged in similar efforts (e.g., [9]–[13]). The majority of the groups working in visual prosthetics today are concentrating either on direct epiretinal [5], [6] (on the front of the retina inside the eye) or subretinal [7], [8] (behind the retina, between the retina and choroid) electrical stimulation, or on less direct stimulation of the retina using a supra-choroidal (behind the choroid, between the choroid and the sclera) or trans-scleral (outside of all or part of the sclera) approach [9]–[11]. For a number of years, our team's approach focused on epiretinal prosthesis design, culminating in the six acute human surgical trials described above, using flexible, polyimide-based stimulating electrode arrays comparable to those in our present design [3], [4]. A number of factors, however, eventually led our group to take an ab externo, subretinal surgical approach to chronic implantation of a wirelessly-driven microstimulator. This design approach yields improved biocompatibility and a less invasive surgery, and it leaves the bulk of the implant device outside the eye.

This work was supported in part by the Boston VA Center for Innovative Visual Rehabilitation, NIH (EY016674-01), NSF (IIS-0515134), the Catalyst Foundation, and the MOSIS Service.

Our first-generation wirelessly-powered implantable retinal stimulation device [1] was implanted in Yucatan minipigs during the spring and summer of 2008. We now describe an improved version of the implant, with the circuits encased in a hermetic titanium enclosure, the coils moved to a more magnetically-favorable position, and easier surgical access for electrode array insertion. We have also performed significantly more testing of our thin-film microfabricated electrode array.

II. Retinal Implant Design and Methods

A. System Description

Our implant system consists of a PXI computer-based controller with a user interface for selecting which electrodes to drive and with which level of current. Data from the computer system are sent to a power amplifier, which then transmits wirelessly to the implant by near-field inductive coupling. Data at 100 Kbps are encoded by amplitude shift keying on a 15.5 MHz carrier. Power is also wirelessly transmitted to the implant using a 125 KHz carrier, and is rectified by the implant to create ±2.5 V power supplies.

Stimulation data are transmitted to the chip by a class A power amplifier with a 15.5 MHz carrier, amplitude shift keyed at a 100% modulation index. Bits were encoded by pulse width modulation, with 30% duty cycle representing a digital 1 and 50% duty cycle representing a digital 0, as shown in Fig. 1. Power was transmitted by a class D power amplifier and a resonant tank with a 125 KHz carrier, and was rectified in the implant by a dual half-wave rectifier, creating anodal and cathodal voltage supplies, clamped by a simple 5.1 V Zener diode. Power and data telemetry has been tested in the laboratory up to a 30 mm separation between primary and secondary coils. This is far greater than is needed in most animal experiments.

A custom integrated circuit [18], shown in Fig. 2 and fabricated in 0.5 µm CMOS, receives and decodes the incoming data and delivers stimulating current to the appropriate electrodes based on the timing of transmitted commands. The chip is capable of delivering up to 930 µA of current per channel at steps of 30 µA. This circuit was designed to be an extremely flexible research tool, and is capable of delivering more current than is needed for this animal work. Currents typically delivered to electrodes ranged from 30 to 120 µA.

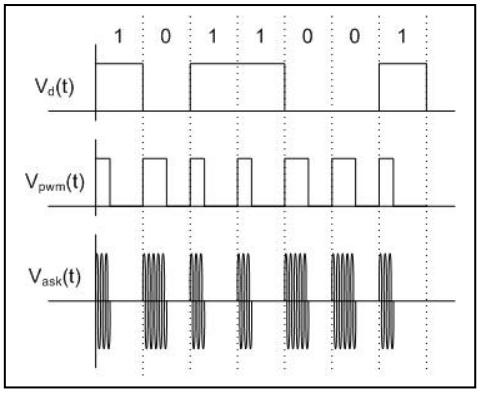

Figure 1. Data are encoded in the carrier by amplitude shift keying (ASK), with pulse width modulation (PWM) encoding of bits. Duty cycle of 30% represents a 1, while 50% represents a 0.

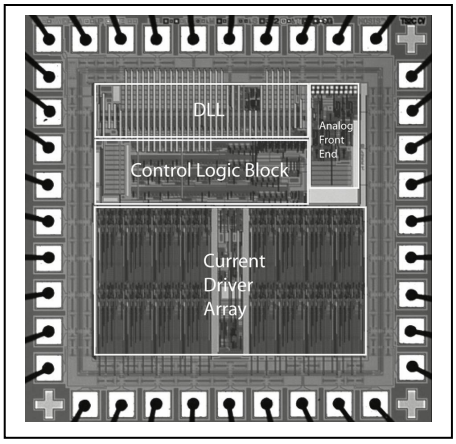

Figure 2. Custom integrated circuit for the retinal prosthesis. This 0.5 µm CMOS chip receives incoming stimulation data, decodes it with a delay locked loop, and delivers the appropriate stimulation currents to electrodes with 15 current sources.

The package containing the chip is attached to the outside of the eye, and its electrical stimulation current is delivered to the retinal nerve cells via a thin-film microfabricated array of sputtered iridium oxide film (SIROF) electrodes, which is surgically inserted into the subretinal space through a flap in the sclera.

B. Differences from First-Generation Device

Our first-generation device [1] was assembled on a flexible substrate that wrapped around the eye inside the socket, attaching to the sclera of the eye (Fig. 3). This device had three significant design drawbacks: (1) small receiver coils made power and data telemetry difficult; (2) the silicone coating held up well in studies of up to 10 months, but would not be viable for chronic trials of 5-10 years; and (3) the required surgical approach for electrode array insertion was very difficult, since the coils were in the way. In addition, we had relatively little data about the long-term survivability of our electrode arrays under continuous stimulation.

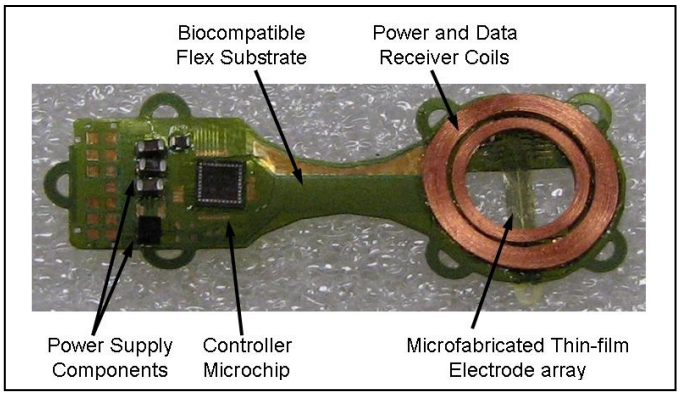

Figure 3. First-generation retinal prosthesis. The flexible implant wraps around the eye, with coils and electrode array in the superior-temporal quadrant and controller circuitry in the superior-nasal quadrant. The prosthesis receives power and data by inductive coupling, and the electrode array accesses the subretinal space via a scleral flap.

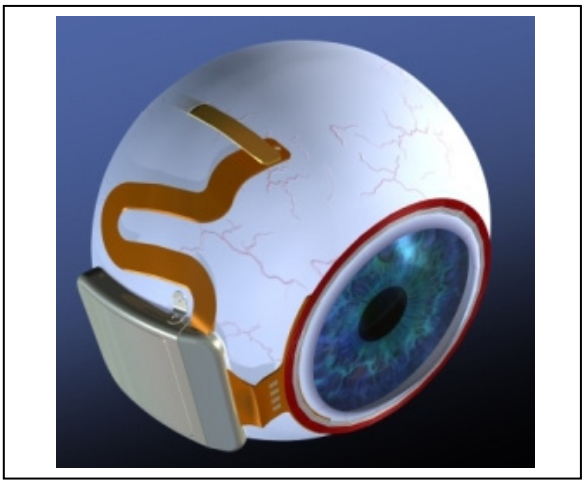

Figure 4. Drawing of hermetic implant concept. The power and data receiver coils rest on the front of the eye, just beneath the conjunctiva. The electronics are encased in a hermetic titanium package, and the electrode array insertion is in its own quadrant, for ease of surgical access.

Our newer-generation device [2] uses the same controller chip [18] and power and data telemetry scheme, but solves the three problems outlined above, with, respectively: (1) larger coils, conforming to the eye, surrounding the cornea, under the conjunctiva; (2) a hermetic, titanium case enclosing the circuitry, attached to the sclera deep in the superior-nasal quadrant; and (3) a serpentine electrode array which extends from the case to the superior-temporal quadrant, giving open surgical access to create the scleral flap and insert the array into the subretinal space. The concept of this hermetic implant is shown in Fig. 4.

C. Improved Implant Components

Relocating the secondary power and data coils from the temporal side of the eye to the anterior of the eye allowed for much larger coils, giving much better inductive coupling. However, these coils rest against the delicate conjunctiva and can wear through and become exposed, creating a risk of infection. To reduce this risk, the coils are carefully wound on a steel sphere so that they match the curvature of the eye. The secondary coils include separate power and data windings and leads, but they are wound together for structural support. They are made of 40 AWG gold wire, with 28 turns for the power coil and two 6-turn coils for a 12-turn center-tapped data receiver. The spherically-molded coil has a mean radius of 9.5 mm and a height off of the eye of less than 0.2 mm. The secondary coils are shown on a model eye in Fig. 5. The primary coils sit in front of the eye, and are made of separate power and data coils in a molded poly(dimethylsiloxane) body. The primary power coil has a mean radius of 19 mm, while the data coil has a mean radius of 12.5 mm. The primary coils are also shown in Fig. 5.

The integrated circuit, which includes the telemetry receiver, digital controller, analog current sources, biases, and startup circuitry, is encased in the titanium enclosure, which measures 11 mm x 11 mm x 2 mm and is curved to conform more closely to the eye. Additionally, Schottky rectifier

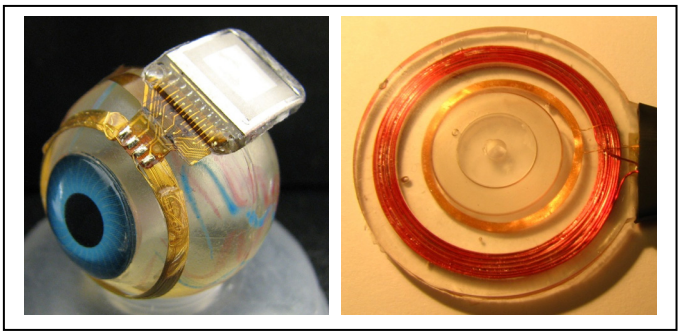

Figure 5. Hermetic retinal prosthesis and associated primary power and data coils. The device on the left is a prototype of the device in Fig. 4. The gold power and data secondary coils are wound on a sphere to match the curvature of the eye. The machined titanium case with welded lid, hermetic feedthrough, and epoxy header protects the internal circuitry. The serpentine electrode array is out of view over the top of the model eye. The primary coils on the right are potted in poly(dimethylsiloxane).

diodes, two power supply capacitors, a discrete resistor and capacitor for power-up reset delay, a resonating capacitor for the power secondary coil, and a 5.1 V Zener diode for power supply regulation are included in the package. The circuit board included in the hermetic package is shown in Fig. 6. The integrated circuit is flip-chip bonded to the board, and all other components are soldered. Ground pads at the two corners opposite the feedthrough pins are soldered to pins in the case, allowing the titanium case to serve as a current return counter electrode for stimulation. Platinum is sputtered onto portions of the case to improve its current-carrying effectiveness.

The novel, serpentine design of our flexible, thin-film 16 µm thick polyimide array of 400 µm diameter SIROF electrodes allows the surgeon to route it behind the superior rectus muscle and insert the electrodes from the superior-temporal quadrant. Since the titanium case is in the superior-nasal quadrant and the secondary coil is low-profile, there is nothing blocking surgical access to the scleral flap. The retina is first separated from the choroid with a bleb of fluid injected from inside the eye, then the array is inserted into the bleb space. The retina slowly settles on top of the array and holds it in place.

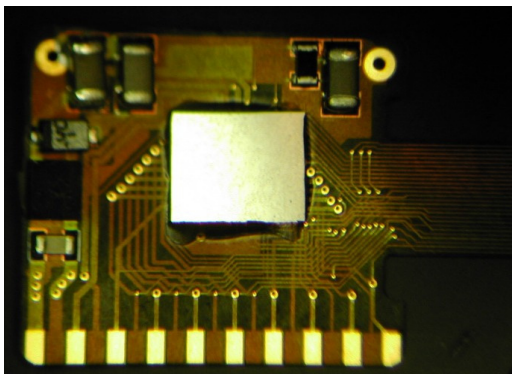

Figure 6. Retinal implant circuit board. The communication, control, and stimulation integrated circuit is attached to the board along with power supply components, and this board is inserted into the curved titanium package. The pads on the bottom are soldered to the hermetic feedthrough pins of the package.

The placement of the electrode array in the subretinal space takes advantage of the eye's natural forces holding the retina against the choroid. The array is sutured to the sclera just outside the point where it enters the eye, but no attachment is necessary in the subretinal space. By contrast, epiretinal electrode placement typically requires one or more retinal tacks to hold the array against the retina.

D. Long-Term Electrode Pulsing

Encasing the electronics in titanium allows this device to be implanted for a much longer time than the first-generation device. This longer-term implantation requires additional testing of the microfabricated SIROF electrodes under chronic pulsing. To assess the stability of these electrodes for chronic animal implantation, we subjected them to long-term in vitro pulsing. Arrays with sixteen 400 μm diameter electrodes were pulsed at 37°C in an inorganic model of interstitial fluid [19]. The multichannel stimulators for the in vitro pulsing employ circuits generating an electrical current pulse protocol similar to that used in the implant for animal testing. Eight electrodes on each array were pulsed at a charge density of 200 $\mu C/cm^2$ (1 ms pulse width, 50 Hz repetition rate) using a 0.6 V Ag/AgCl interpulse bias [20].

E. Implant Testing

The full implant system was tested dry on the bench, as well as in vitro in a phosphate buffered saline solution. On the lab bench, dry testing was performed by connecting to the device though a test tail. Electrode loads, each consisting of a resistor in series with a parallel resistor-capacitor pair, were attached to the current source outputs. Balanced biphasic current pulses ranging from 30 to 240 μA were delivered with pulse durations of 1 ms. The load voltage was directly measured and recorded during wireless operation of the device.

During in vitro testing, the device was attached to a model eye and submerged in a saline bath. Electrodes were driven with balanced biphasic pulses of current, 30-240 μA at 1 ms pulse width per phase (24-192 $\mu C/cm^2$). Similar stimulation parameters were used during in vivo stimulation trials performed in two Yucatan minipigs. Electrode voltage was recorded via the test tail used in bench tests. The test tail was then cut off in preparation for implantation in the minipig. The device was retested in the bath. Without the test tail, less-direct measurements of implant function were required. Needle electrodes were immersed in the saline, and the differential voltage was measured with a custom-built instrumentation amplifier. To ensure that the device was working in the pig eye, the same type of measurement was made in vivo with a contact lens electrode on the eye surface and an ear reference electrode. These measurements were entirely non-invasive and were meant to show continued function of the implant over time. We did not test any response from the minipig's visual system. While it is common to test electrically-evoked responses in the visual cortex of an animal, as we have done in rabbits in the past [21], it is logistically difficult to record these signals in the pig in an acute experiment and tremendously difficult to do so chronically. We determined that there was not enough to be learned from electrically-evoked response recordings to justify the effort.

Figure 7. Photo of the retinal surgeon implanting a hermetic prosthesis onto the minipig eye. The molded gold telemetry coil surrounds the cornea, while the titanium hermetic case containing the custom stimulation electronics is attached to the sclera.

The devices were implanted in two minipigs, each weighing roughly 20 kg. Electroretinograms (ERGs) were taken pre-operatively to assess the general health of each pig's retina, and they were also taken at the beginning of subsequent exams. The conjunctiva was resected, and a bleb was raised with a needle from the front of the eye to lift the retina off of the choroid. Next, the prosthesis was attached to the sclera, and a flap was made through the sclera for the insertion of the electrode array into the subretinal space. The array was inserted through the scleral flap and through a choroidal incision into the subretinal space. The external portion of the array was sutured into place, and the conjunctiva was sutured back over the implant. The device on the pig eye is shown in Fig. 7.

The contact lens electrode was placed on the pig's eye, and two electrodes were placed on the ears. A differential measurement was made between the contact lens electrode and one of the ear electrodes, while the second ear electrode served as a reference voltage for the differential amplifier circuit. The primary telemetry coils were then placed near the front of the eye and held in place by the surgeon. Power and data were delivered to the implant and adjusted until the recording electrode showed stimulus artifact from the pulsing current sources of the implant.

Follow-up exams were conducted on the animals one week after implantation and approximately every three to four weeks thereafter. These exams took place in the surgical facility but were non-sterile procedures. The pig was anesthetized and ERG recordings were taken. The contact lens electrode, ear reference electrodes, and primary power and data coils were placed by the surgeon. Power and data were delivered to the implant and the stimulus artifact was recorded as in the original surgery.

III. RESULTS

A. Long-Term Electrode Pulsing

An example of the voltage transients from eight electrodes on one array and a representative current waveform are shown in Fig. 8. The voltage transients are quite similar for the eight electrodes with maximum cathodal potential (Emc) of about 0.4 V Ag|AgCl, well positive of the –0.6 V water reduction potential on SIROF. Cyclic voltammetry in the model-ISF also showed a consistency in electrode response and good stability

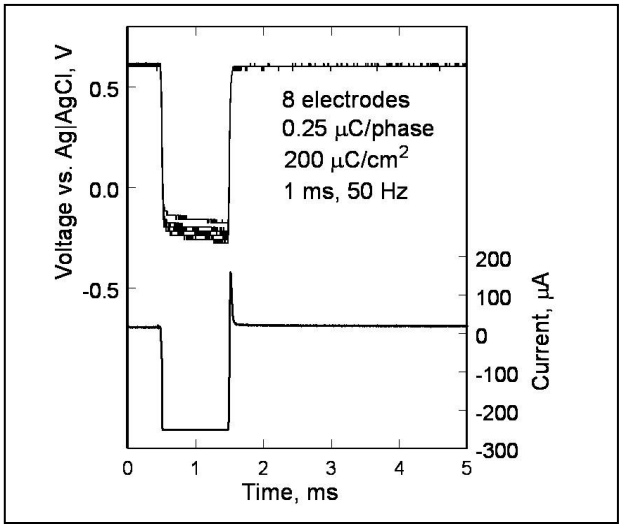

Figure 8. Voltage transients of eight SIROF electrodes on a polyimide array. The electrodes have been pulsed for 2900 hours at 200 μC/cm^2. A sample current waveform is also shown.

over long-term pulsing. In Fig. 9, the voltammagrams of the eight pulsed electrodes are compared after 670 hours and 2900 hours of pulsing. The cause of the observed changes in the CV response between 670 hours and 2900 hours is unclear, although the observed changes would be consistent with a decrease in the density of the SIROF due to hydration.

B. Implant in Vitro and in Vivo Testing

A typical electrode in vitro test waveform is shown in Fig. 10. The RF power and data waveforms are visible in the figure. Also note the step-ramp shape of the electrode voltage waveform. Recall that bench tests of the prosthesis used a resistor in series with a resistor-capacitor pair as a model electrode load. A current pulse through a series resistor and capacitor yields a characteristic step-ramp waveform. The additional resistor in parallel with the capacitor serves to curve the ramp slightly. The electrode voltage waveform in Fig. 10 shows not only the step from the resistive portions of the fluid and the electrode access resistance, but also the ramp from the charging of the electrode-tissue interface.

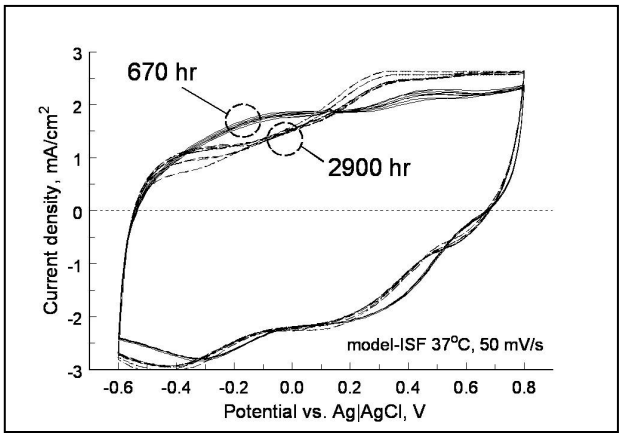

Figure 9. Cyclic voltammagrams of eight SIROF electrodes after 670 hours (solid) and 2900 hours (dashed) of pulsing at 200 μC/cm^2.

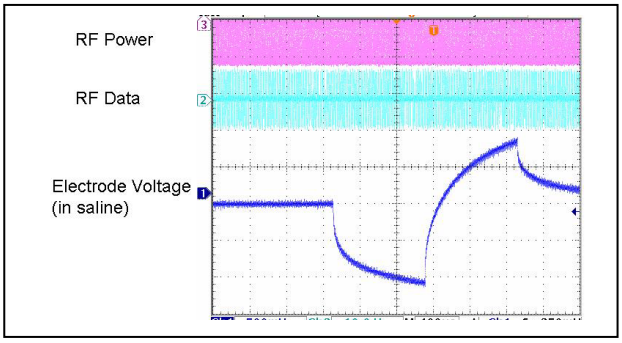

Figure 10. In vitro electrode test waveform for a wirelessly-driven implant. The bottom waveform shows the electrode waveform in saline, measured via a test tail which is trimmed off before surgery.

Recorded stimulus artifact waveforms from stimulation of the minipig eye are shown in Fig. 11. Because of the measurement setup, these waveforms show only the resistive voltage of current flowing through fluid. The capacitive ramp in Fig. 10 shows charge buildup at the electrode-tissue interface, which is not measured by the contact lens electrode. The waveforms in Fig. 11 show a great deal of variation, largely due to inconsistencies in the placement of the contact lens electrode and the use of a distant reference electrode on the ear. With the reference electrode on the ear, well outside the field distribution from the electrode, the contact lens voltage is measured with respect to the pig's body potential. The measurement electrode is placed on the cornea, which we believe may be near the center of the field distribution, where the potential is nearly equal to the pig's body potential. Our amplifiers can show small differences in potential, but inconsistent placement, or even movement, of the contact lens electrode can result in drastic changes of the size of the measured stimulus artifact waveforms. However, the goal of this measurement is to show the existence, not the amplitude, of stimulus artifact, and when the artifact waveform is present, it is unmistakable. We have performed control tests with the RF transmitters on but commanding zero-current pulses, and we have seen no stimulus artifact [1]. This method of artifact measurement was non-invasive, and it greatly simplified the testing, allowing for non-sterile follow-up studies after surgical implantation of the device.

In both minipigs, the conjunctiva over the device wore through and caused exposure of the coils and case. This required explantation of the devices, one after three months and one after five and a half months. A number of factors may have caused this exposure. The coil edge met the conjunctiva at an angle that may have caused tension in the thin conjunctiva. The winding radius of the coil has been changed to correct this. Also, it was thought that the hermetic case was too far anterior, and was increasing the tension in the conjunctiva, or that the case was being pushed forward by movement of the eye in the socket. The first concern was addressed by redesigning the flex circuit connecting the coil and the case, placing the case farther back in the socket. The second concern was addressed by redesigning the way the case is sutured to the eye, with various different shapes of suture tabs to ensure that the case remains in place. This development effort is still underway.

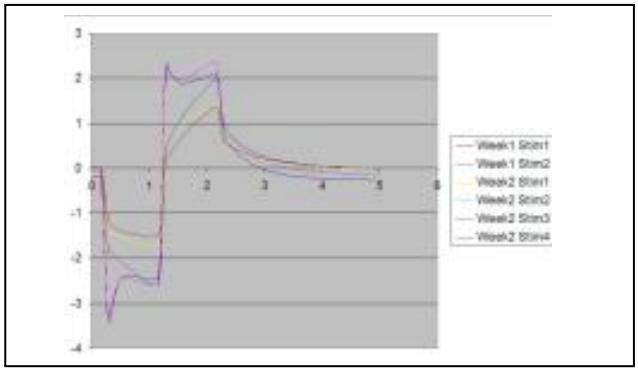

Figure 11. Measured electrical stimulus artifact from the minipig eye. Variation in waveform size is thought to be a result of variation in electrode position on the eye.

IV. Conclusion

A hermetic, wirelessly-driven retinal prosthesis device has been developed and built. It has been tested both in saline environments and in two Yucatan minipigs. Operation of the implant has been verified in the minipig eye for up to five and a half months. The device presented here is capable of being implanted for a much longer time than our previous PDMS-coated device. This allows for the 10-year survivability expected by the FDA for clinical trials. While our implant worked reliably during animal testing for three months in one minipig and five and a half months in another, exposure problems at the conjunctiva forced an early end to both experiments. We have slightly redesigned the coil molding process and the connection between the case and the coil to ease the tension on the conjunctiva for future trials. These modifications will allow longer-term animal implantation trials in the near future, with a view toward human clinical trials and the ultimate goal of a subretinal prosthesis capable of restoring useful vision to blind patients.

Acknowledgment

The authors acknowledge technical support and assistance from O. Mendoza, T. Plante, S. Behan, J. Dumser, G. Swider, B. Yomtov, and J. Loewenstein, as well as administrative support from K. Quinn and P. Davis. The authors acknowledge C. Pina and MOSIS for in-kind foundry services in support of their research.

References

[1] D. B. Shire, et al., "Development and Implantation of a Minimally-Invasive, Wireless Sub-Retinal Neurostimulator," IEEE Trans. Biomed. Eng., accepted for publication in March, 2009.

[2] S. K. Kelly, et al., "Realization of a 15-Channel, Hermetically-Encased Wireless Subretinal Prosthesis for the Blind," Proc. IEEE Engineering in Medicine and Biology Conference, pp. 200-203, 2009.

[3] J. F. Rizzo III, J. Wyatt, J. Loewenstein, S. Kelly, and D. Shire, "Perceptual Efficacy of Electrical Stimulation of Human Retina with a Microelectrode Array During Short-Term Surgical Trials," Invest. Ophthalmol. Vis. Sci., vol. 44, pp. 5362-5369, 2003.

[4] J. F. Rizzo III, J. Wyatt, J. Loewenstein, S. Kelly, and D. Shire, "Methods and Perceptual Thresholds for Short-Term Electrical Stimulation of Human Retina with Microelectrode Arrays," Invest. Ophthalmol. Vis. Sci., vol. 44, pp. 5355-5361, 2003.

[5] D. Yanai, et al., "Visual Performance Using a Retinal Prosthesis in Three Subjects with Retinitis Pigmentosa," Am. J. Ophthalmol., vol. 143, pp. 820-827, 2007.

[6] H. Gerding, F. P. Benner, and S. Taneri, "Experimental Implantation of Epiretinal Retina Implants (EPI-RET) With an IOL-Type Receiver Unit," J. Neural Eng., vol. 4, pp. S38-S49, 2007.

[7] P. J. DeMarco, et al., "Stimulation via a Subretinally Placed Prosthetic Elicits Central Activity and Induces a Trophic Effect on Visual Responses," Invest. Ophthalmol. Vis. Sci., vol. 48, pp. 916-926, 2007.

[8] T. Schanze, H. G. Sachs, C. Wiesenack, U. Brunner, and H. Sailer, "Implantation and Testing of Subretinal Film Electrodes in Domestic Pigs," Exp. Eye Res., vol. 82, pp. 332-340, 2006.

[9] J. A. Zhou, et al., "A Suprachoroidal Electrical Retinal Stimulator Design for Long-Term Animal Experiments and In-Vivo Assessment of Its Feasibility and Biocompatibility in Rabbits," J. Biomed. Biotech., vol. 2008, Article ID 547428, 10 pp., 2008.

[10] Y. T. Wong, et al., "Retinal Neurostimulator for a Multifocal Vision Prosthesis," IEEE Trans. Neural Syst. Rehab. Eng., vol. 15, pp. 425-434, 2007.

[11] Y. Terasawa, et al., "The Development of a Multichannel Electrode Array for Retinal Prostheses," J. Artif. Organs, vol. 9, pp. 263-266, 2006.

[12] R. Hornig, et al., "The IMI Retinal Implant System," in M. S. Humayun, J. D. Weiland, G. Chader, and E. Greenbaum, eds., Artificial Sight: Basic Research, Biomedical Engineering, and Clinical Advances, New York: Springer, pp. 111-128, 2007.

[13] E. Zrenner, "Restoring Neuroretinal Function: New Potentials," Doc. Ophthalmol., vol. 115, pp. 56-59, 2007.

[14] D. Friedman, et al., "Prevalence of Age-Related Macular Degeneration in the United States," Arch. Ophthalmol., vol. 122, pp. 564-572, 2004.

[15] R. E. Marc, et al., "Neural Reprogramming in Retinal Degenerations," Invest. Ophthalmol. Vis. Sci., vol. 48, pp. 3364-3371, 2007.

[16] R. J. Jensen and J. F. Rizzo III, "Responses of Ganglion Cells to Repetitive Electrical Stimulation of the Retina," J. Neural Eng., vol. 4, pp. S1-S6, 2007.

[17] S. K. Kelly, "A System for Electrical Retinal Stimulation for Human Trials," M.Eng. Thesis, MIT, 1998.

[18] L. S. Theogarajan, "A Low-Power Fully Implantable 15-Channel Retinal Stimulator Chip," IEEE J. Solid-State Circuits, vol. 43, pp. 2322-2337, 2008.

[19] S. F. Cogan, P. R. Troyk, J. Ehrlich, C. M. Gasbarro, and T. D. Plante, "The Influence of Electrolyte Composition on the In Vitro Charge-Injection Limits of Activated Iridium Oxide (AIROF) Stimulation Electrodes," J. Neural Eng., vol. 4, pp. 79-86, 2007.

[20] S. F. Cogan, P. R. Troyk, J. Ehrlich, and T. D. Plante, "In Vitro Comparison of the Charge-Injection Limits of Activated Iridium Oxide (AIROF) and Platinum-Iridium Microelectrodes," IEEE Trans. Biomed. Eng., vol. 52, pp. 1612-1614, 2005.

[21] H. A. Shah, S. R. Montezuma, and J. F. Rizzo III, "In Vivo Electrical Stimulation of Rabbit Retina: Effect of Stimulus Duration and Electric Field Orientation," Exp. Eye Res., 83 (2), pp. 247-254, 2006.